

New Transmission-Selective Antimalarial Agents through Hit-to-Lead Optimization of 2-([1,1'-Biphenyl]-4-carboxamido)benzoic Acid Derivatives

Janette Reader,^[a] Daniel F. L. Opperman,^[a] Mariëtte E. van der Watt,^[a, b] Anjo Theron,^[c] Meta Leshabane,^[a] Shanté da Rocha,^[a] Jonathan Turner,^[d] Kathleen Garrabrant,^[d] Ivett Piña,^[d] Catherine Mills,^[d] Patrick M. Woster,^[d] and Lyn-Marié Birkholtz*^[a]

Malaria elimination requires multipronged approaches, including the application of antimalarial drugs able to block human-to-mosquito transmission of malaria parasites. The transmissible gametocytes of *Plasmodium falciparum* seem to be highly sensitive towards epidrugs, particularly those targeting demethylation of histone post-translational marks. Here, we report exploration of compounds from a chemical library generated during hit-to-lead optimization of inhibitors of the human histone lysine demethylase, KDM4B. Derivatives of 2-([1,1'-biphenyl]-4-carboxamido) benzoic acid, around either the amide or a sulfonamide linker backbone (2-(arylcabox-

amido)benzoic acid, 2-carboxamide (arylsulfonamido)benzoic acid and *N*-(2-(1*H*-tetrazol-5-yl)phenyl)-arylcarboxamide), showed potent activity towards late-stage gametocytes (stage IV/V) of *P. falciparum*, with the most potent compound reaching single digit nanomolar activity. Structure-activity relationship trends were evident and frontrunner compounds also displayed microsomal stability and favourable solubility profiles. Simplified synthetic routes support further derivatization of these compounds for further development of these series as malaria transmission-blocking agents.

Introduction

Small molecules targeting chromatin remodelling enzymes, so called 'epidrugs', have been explored for their ability to prevent cellular replication events. Epigenetic modulating compounds typically affect histone modifying enzymes and DNA methylases/demethylases and thereby affect the non-sequence dependent but heritable phenotypes associated with epigenetic

regulation. Epidrugs can, for instance, inhibit either 'writers' (e.g. methyltransferases or acetyltransferases) or 'erasers' (e.g. demethylases or de-acetylases) of histone post-translational modifications, which results in altered chromatin status and gene expression. In some disease states, dysregulation of epigenetic enzymes leads to aberrant gene expression, and eventually cell death.^[1] As antineoplastics,^[2] epidrugs like azacitidine, decitabine, vorinostat and romidepsin,^[3] have been approved for clinical use, with several others currently in human clinical trials.^[4]

The malaria parasite, *Plasmodium falciparum*, has a complex life cycle with phases associated with both development in the human host and mosquito (*Anopheles*) vector. Pathology in humans is associated with massive population expansion due to asexual replication of the parasite in the erythrocyte compartment every 48 h. Disease transmission, on the other hand, is entirely dependent on the parasite's sexual gametocyte forms, with mature (stage V) male and female gametocytes being the only forms able to sustain transmission from the human host to the mosquito vector. Due to the low numbers of parasites required to sustain transmission, these stages are favourable targets for chemotherapeutic intervention.^[5,6] The sexual developmental processes of the parasite relies heavily on epigenetic mechanisms^[7-12] and the parasite genome encodes the required complement of histone modifying enzymes affecting histone acetylation and methylation, protein arginine methyltransferases, and histone lysine demethylases^[13] in addition to other non-histone epigenetic modifiers. As a result, inhibitors of histone modifying enzymes have been investigated as novel chemotypes in antimalarial drug discovery efforts.^[14-22] Despite the fact that these investigations were primarily focussed on

[a] J. Reader, D. F. L. Opperman, M. E. van der Watt, M. Leshabane, S. da Rocha, L.-M. Birkholtz
Department of Biochemistry, Genetics and Microbiology
Institute for Sustainable Malaria Control
University of Pretoria; Lynnwood Road
Pretoria, 0028 (South Africa)
E-mail: lbirkholtz@up.ac.za

[b] M. E. van der Watt
School of Health Systems and Public Health
University of Pretoria, Hatfield, Pretoria 0028 (South Africa)

[c] A. Theron
Next Generation Health
Council for Scientific and Industrial Research
Pretoria 0001 (South Africa)

[d] J. Turner, K. Garrabrant, I. Piña, C. Mills, P. M. Woster
Department of Drug Discovery and Biomedical Sciences
Medical University of South Carolina
Charleston, SC 29425 (USA)

Supporting information for this article is available on the WWW under <https://doi.org/10.1002/cbic.202200427>

This article belongs to the Joint Special Collection "Biological and Medicinal Chemistry in Africa".

© 2022 The Authors. ChemBioChem published by Wiley-VCH GmbH. This is an open access article under the terms of the Creative Commons Attribution Non-Commercial License, which permits use, distribution and reproduction in any medium, provided the original work is properly cited and is not used for commercial purposes.

asexual *P. falciparum* parasites, epigenetic inhibitors were recently shown to be highly effective against gametocyte stages,^[23–26] with the implication that these compounds could be used in malaria elimination strategies by blocking transmission.^[5,26] In both life cycle forms, epidrugs disturb gene expression leading to cell death.^[21,22,26,27]

Although the majority of epigenetic inhibitors target histone deacetylation (histone deacetylase, HDAC inhibitors) or DNA methyltransferase, inhibitors of histone methyltransferases and lysine demethylases are the largest group of epidrugs in clinical investigation.^[28] Histone methylation (at either lysine or arginine residues) is a key chromatin modification associated with varied functional outcomes depending on the level of methylation (e.g. mono-, di- or trimethylation). Interfering with these processes therefore results in more nuanced phenotypic effects. As such, preventing removal of methylation marks (by inhibiting histone demethylases) is particularly effective. The histone lysine demethylase (KDM) family contains two catalytically distinct classes: 1) the FAD⁺-dependent lysine-specific demethylases (LSD, KDM1 subfamily), and 2) the α -ketoglutarate (α -KG or 2-oxaloglutarate) and Fe²⁺-dependent jumonji-domain containing demethylases (JMJD).^[29] The latter includes KDM4 family members, which demethylate important repressive marks such as H3K9me2/3 and H3K36me2/3, and when overexpressed, such as in cardiovascular diseases and multiple cancers,^[29] promote aberrant gene expression. *P. falciparum* parasites contain three JMJD members and the one lysine-specific demethylase (LSD1), with *PfJmJ*C1 active on H3K9me2/3 and also H3K36me3, with *PfJmJ*3 specific for the latter.^[25,30] Importantly, these parasitic epigenetic enzymes are structurally distinct from the corresponding human enzymes, making them attractive drug targets.

ML324 (*N*-(3-(dimethylamino)propyl)-4-(8-hydroxyquinolin-6-yl)benzamide (1, Figure 1), is a small molecule inhibitor targeting KDM4E^[31] and KDM4B.^[28,32] This compound inhibits Herpes simplex virus and cytomegalovirus replication,^[33] and has potent transmission-blocking activity in *P. falciparum*.^[26] In

this parasite, ML324 specifically targets mature gametocytes at low nanomolar potencies, blocks the formation of male gametes and dramatically reduces oocyst formation in the mosquito.^[26] This is due of accumulation of H3K9me3 and silencing of genes required for transmission processes.^[26] Similar to other well-established inhibitors of *JmJ*C including JIB-04, ML324 is able to inhibit *PfJmJ*3 particularly by preventing iron coordination and thereby catalytic activity.^[25] *PfJmJ* proteins contain all the conserved catalytic residues for α -KG, Fe²⁺ and substrate binding.

While ML324 exhibits good cell permeability, solubility and microsomal stability,^[31] its hydroxyquinoline moiety could have off-target iron chelating capabilities, and its development is compromised by complex synthetic pathways.^[31] Because of this, we sought to identify novel scaffolds with the potential to inhibit KDM4B, by combining consensus computational docking data to identify a dramatisable scaffold with KDM4B inhibitory action with 2-([1,1'-biphenyl]-4-carboxamido) benzoic acid (2, Figure 1) as starting point. We report here the identification of novel analogues based on 3 similar chemical scaffolds, 2-(arylcaboxamido)benzoic acid (2), *N*-(2-(1*H*-tetrazol-5-yl)phenyl)-arylcaboxamide (3) and 2-(arylsulfonamido)benzoic acid (4), and their *in vitro* activity against multiple life cycle stages of *P. falciparum*, including confirmation of transmission-blocking activity and exploration of their possible target in these parasites. These data provide a basis for performing hit-to-lead optimization of highly active compounds with the goal of establishing structure-activity relationships for antimalarial activity. In addition, our long-term goal is to identify compounds to advance to the clinic as a new class of antimalarial agents.

Results and Discussion

Preparation of derivatives

All 2-(arylcaboxamido)benzoic acid, 2-(arylsulfonamido)benzoic acid and *N*-(2-(1*H*-tetrazol-5-yl)phenyl)-arylcaboxamide derivatives were synthesized as previously described.^[34] All intermediates and target compounds were purified by silica gel or C18 column chromatography. Pure intermediates and final products were fully characterized by NMR and LC-MS analysis. Purity of intermediates and final products was determined by UPLC analysis, and final compounds were $\geq 95\%$ pure by UPLC prior to use in biological studies.

Evaluation of the structure-activity relationship for *in vitro* antiplasmodial activity of the amide linker derivatives

Since prior evidence suggested a selective action of the *jmj* demethylase inhibitors, ML324^[26,35] and JIB-04^[35] on late-stage gametocytes (> 95% stage IV/V), the structure-activity relationships of compound 2 derivatives were explored. Three derivatives of 2, compounds 7, 8 and 16, displayed potent (< 100 nM) activity against late-stage gametocytes (Table 1).

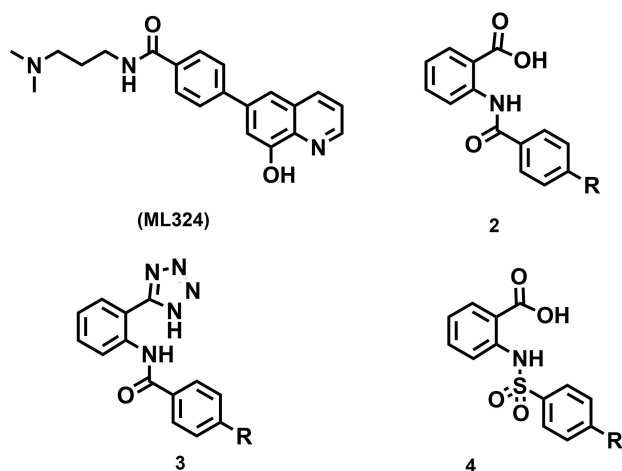
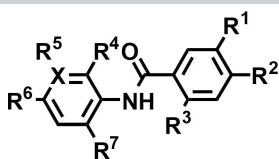
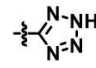
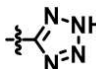
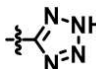


Figure 1. ML324 (1) and the novel, dramatisable 2-(aryl-4-carboxamido)benzoic acid (2), *N*-(2-(1*H*-tetrazol-5-yl)phenyl)-arylcaboxamide (3) and 2-(arylsulfonamido)benzoic acid (4) scaffolds.

Table 1. Derivatives of compound 2 with changes around the amide core.



Cmpd	R ¹	R ²	R ³	R ⁴	R ⁵	R ⁶	R ⁷	X	NF54 gametocyte IC ₅₀ [nM] ^[a]	cLogP ^[b]
DHA 1 (ML324)									87.70 ± 3.7 ^[c] 74.18 ± 8.27	3.40
5	H	C ₆ H ₅	H	H	H	H	COOH	C	514 ± 66	5.21
6	H		H	CH ₃	H	H	COOH	C	1142 ± 28	5.05
7	H		H	H	H	F	COOH	C	9.34 ± 1.43	5.47
8	H		H	F	H	H	COOH	C	77.19 ± 9.64	4.87
9	H		H	H	F	H	COOH	C	104.7 ± 18	5.47
10	C ₆ H ₅	H	H	CH ₃	H	H	COOH	C	665 ± 56	5.05
11		H	H	F	H	H	COOH	C	> 10000	4.87
12	H	H	C ₆ H ₅	H	H	H	COOH	C	> 10000	4.75
13	H	H		CH ₃	H	H	COOH	C	> 10000	4.59
14	H	H		H	H	F	COOH	C	674 ± 179	5.01
15	H	H		H	F	H	COOH	C	> 10000	5.01
16	H	H	4-CH ₃ -(C ₆ H ₅)	CH ₃	H	H	COOH	C	55.13 ± 10.33	5.01
17	H	H	2-CH ₃ O-(C ₆ H ₅)	CH ₃	H	H	COOH	C	> 10000	3.99
18	H	4-F-(C ₆ H ₅)	H	H	H	H	COOH	C	> 10000	5.37
19	H	4-CF ₃ -(C ₆ H ₅)	H	H	H	Br	COOH	C	291.8 ± 28	7.08
20	H		H	H	F	F	COOH	C	527.9 ± 61	6.47
21	H		H	H	H	Br		C	370.5 ± 57	5.03
22	H	C ₆ H ₅	H	H	-	H	COOH	N	634.4 ± 24	4.69
23	C ₆ H ₅	H	H	H	-	H	COOH	N	583.1 ± 49	4.69
24	H	3-CH ₃ -(C ₆ H ₅)	H	H	-	H	COOH	N	> 10000	5.19
25	H	4-F-(C ₆ H ₅)	H	H	-	H	COOH	N	> 10000	4.84
26	C ₄ H ₄		H	H	-	H	COOH	N	> 10000	3.97
27	H	C ₆ H ₁₁	H	H	F	F	COOH	C	> 10000	6.31
28	C ₄ H ₄		H	H	F	H	COOH	C	> 10000	4.75
29	H		H	H	H	CH ₃		C	> 10000	4
30	H	4-CH ₃ -(C ₆ H ₅)	H	H	H	CF ₃		C	> 10000	4.83

[a] Activity against late-stage (stage IV/V) gametocytes of three independent biological repeats, each in technical triplicates, mean ± S.E. indicated. [b] Predicted cLogP from Chemdraw. [c] As published in Reader *et al.* 2022.^[38]

Some initial changes to the benzoic acid ring system of **2** at positions R⁴, R⁵ and R⁶ included methylation of the aromatic ring (compounds **6**, **10**, **13**, **17** and **29**), which resulted in sharp decreases in antimalarial activity. In addition, methylation of the benzoic acid moiety at R₄ combined with addition of a 4-trifluoromethylphenyl at R³ also increased activity, as in **16**. Conversion of the benzoic acid to a 4-pyridine carboxylic acid produced **22**–**26**, which supported late-stage gametocytocidal activity (**22**; 634 nM), even when the distal phenyl was moved from *para* to *meta* position (**23**; 583 nM). Changing the benzoic acid to a naphthalene (**27**; > 10 μM) or phenylcyclohexane (**28**; > 10 μM), was however, not tolerated. Halogenation of the benzoic acid produced the most positive outcome. Addition of a fluorine at R⁴, R⁵ or R⁶ led to a significant increase in activity (compounds **7**, **8** and **9**). The most potent compound overall, (**7**; 9.34 ± 1.94 nM on late-stage gametocytes) contained a fluorine group at position R⁶ of the benzoic acid (Table 1). This fluorination seems essential to activity, with loss thereof resulting in a 54-fold drop in gametocytocidal activity as observed in the unfluorinated benzoic acid, **5** (IC₅₀ at 515 nM). Compound **5** therefore represents the minimum pharmaco-

phore for the 2-([1,1'-biphenyl]-4-carboxamido) benzoic acid scaffold. Movement of the fluorine around the benzoic acid ring was somewhat tolerated with minimal loss in activity (**9**; 104.7 nM), but was entirely dependent on the *para* positioning of the distal phenyl in the biphenyl moiety, with changes in this position leading to a complete loss in activity as in **11** (> 10 μM) compared to **8** (77 nM). It is important to note that the addition of a fluorine is often used to improve the permeability of drugs by e.g. increasing lipophilicity and addressing oxidative metabolism.^[36] Fluorinated derivatives indeed displayed higher predicted cLogP values. Combined with the enhanced permeability of late-stage gametocytes with a ghost-like erythrocyte and the expression of perforin-like proteins^[37] fluorination might be a contributor to the improved efficacy of these derivatives.

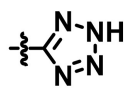
Based on the above observations, we sought to investigate additional positions of the terminal phenyl located at R². Activity was somewhat maintained with *meta* positioning of the distal phenyl, but only for the methylated benzoic acid, **10** (665 nM). Movement of the distal phenyl to the *ortho* position was somewhat tolerated, however as for **7**, this was still dependent on the position of the benzoic acid fluorine (**14**;

674 nM vs. **15**; > 10 μ M). We next interrogated substitution at the R² phenyl group. Methylation of the distal phenyl dramatically increased potency (**16**; 55 nM) whereas the addition of a methoxy group led to a complete loss in activity (**17**; > 10 μ M). Additional substitution of the biphenyl moiety, such as fluorination of the terminal phenyl, was not tolerated (**18**; > 10 μ M), however, increasing the polarity at this position with a trifluoromethyl group increased activity up to 34-fold for the 3-bromobenzoic acid (**19**; 292 nM). Activity was also maintained with the additional replacement of the carboxyl moiety with a tetrazole group (**21**, 371 nM). The latter substitution though, was detrimental in the absence of a halogenation (**29** and **30**; > 10 μ M), again supporting the above observations with regards to fluorination events.

Evaluation of *in vitro* antiplasmodial activity of the sulfonamide linker

Changing the amide core to a sulfonamide resulted in an overall less potent activity profile compared to the amides (Table 2). The sulfonamide matched pair of **5**, the minimum pharmacophore for this series, displayed equipotent activity compared to its amide partner **31** (IC₅₀ at 533 nM, Table 2). This implies that at least for direct comparison of these two compounds, the nature of the linker does not influence activity. Fluorination of the benzoic acid again played an important role in efficacy, mediating activity of compounds such as **33** and **34** (439 vs 647 nM, respectively) but only in the presence and position of the methyl group at R⁶ or R⁵, respectively. Bromination of the benzoic acid was also tolerated (**36**; 780 nM), but with the similar prerequisite of lack of benzoic acid methylation. The addition of a trifluoromethyl to the phenyl at R² in the sulfonamide series abrogated activity, in contrast to what was observed for the amide backbone. Any

Table 2. Exploration of the sulfonamide core.

Cmpd	R ¹	R ²	R ³	R ⁴	R ⁵	R ⁶	R ⁷	X	NF54 gametocyte IC ₅₀ [nM] ^[a]	cLogP ^[b]
DHA 1 (ML324)									87.70 ± 3.7 ^[c] 74.18 ± 8.27	3.40
31	H	C ₆ H ₅	H	H	H	H	COOH	C	533.4 ± 44	5.07
32	H	3-CH ₃ -C ₆ H ₅	H	H	H	CH ₃	COOH	C	746.2 ± 194	6.06
33	H		H	H	H	F	COOH	C	439 ± 93	5.81
34	H		H	H	F	H	COOH	C	646.9 ± 52.4	5.81
35	H	4-CH ₃ -C ₆ H ₅	H	H	F	H	COOH	C	5064 ± 216	5.81
36	H		H	H	Br	H	COOH	C	779 ± 115	6.53
37	H	4-CH ₃ O-C ₆ H ₅	H	H	H	CF ₃	COOH	C	806.5 ± 51.2	6.16
38	H		H	H	H	OCH ₃	COOH	C	> 10000	5.05
39	H	4-Cl-C ₆ H ₅	H	H	H	Br	COOH	C	> 10000	6.75
40	H		H	H	H	OCH ₃	COOH	C	> 10000	5.81
41	H		H	H	H	OCH ₃		C	> 10000	4.73
42	H		H	H	H	CH ₃	COOH	C	> 10000	6.30
43	H	4-F-C ₆ H ₅	H	H	H	F	COOH	C	> 10000	5.46
44	H	C ₆ H ₁₁	H	H	H	CF ₃	COOH	C	> 10000	6.3
45	H		H	H	H	F	COOH	C	> 10000	6.03
46	H	4-CF ₃ -C ₆ H ₅	H	H	H	F	COOH	C	> 10000	6.2
47	H		H	H	F	H	COOH	C	> 10000	6.2
48	H		H	H	H	CH ₃	COOH	C	> 10000	6.48
49	H		H	H	H	OCH ₃	COOH	C	> 10000	5.98
50	H		H	H	CH ₃	H	COOH	C	> 1000	6.48
51		C ₄ H ₈	H	H	H	F	COOH	C	> 10000	5
52		C ₄ H ₄	H	H	H	F	COOH	C	> 10000	4.6
53			H	H	F	H	COOH	C	> 10000	4.6
54			H	H	H	CH ₃	COOH	C	> 10000	4.85
55		O ₂ C ₂ H ₄	H	H	H	H	COOH	C	> 10000	3.26
56			H	H	H	F	COOH	C	> 10000	3.45
57			H	H	F	H	COOH	C	> 10000	3.45
58				H	H	CH ₃	COOH	C	> 10000	3.76

[a] Activity against late-stage (stage IV/V) gametocytes of three independent biological repeats, each in technical triplicates, mean ± S.E. indicated. [b] Predicted cLogP from Chemdraw. [c] Data as published in Reader *et al.* 2022.^[38]

Table 3. Additional *in vitro* life cycle stage profiling and selectivity of the gametocyte active ($IC_{50} < 600$ nM) compounds.

Cmpd	NF54 ABS PB ^[a] IC_{50} [nM]	NF54 ABS SG ^[b] [% inhibition @ 10 μ M]	NF54 male gamete ^[c] [% inhibition @ 2 μ M]	HepG2 [% inhibition @ 50 μ M]
1 (ML324) ^[d]	> 6000	3.854 μ M IC_{50}	93 \pm 2.0	$IC_{50} > 50$ μ M
16	> 10000	8.4	55.0 \pm 10.4	6.7
5	> 10000	10.4	34.7 \pm 5.8	12.3
7	> 10000	12.7	43.5 \pm 6.6	5.6
8	> 10000	6.4	38.8 \pm 21.6	4.4
9	> 10000	17.2	13.8 \pm 2.1	20.0
10	ND		31.8 \pm 5.0	ND
19	ND		0 \pm 5.4	ND
21	ND		24.1 \pm 9.9	ND
33	> 10000	11.9	41.8 \pm 5.0	ND
31	> 10000	9.2	50.8 \pm 7.0	ND

[a] *P. falciparum* NF54 drug sensitive asexual blood stage parasites (ABS) tested on the PrestoBlue assay, $n = 3$. [b] *P. falciparum* NF54 drug sensitive asexual blood stage parasites (ABS) tested on the SYBR Green I proliferative assay, $n = 3$. [c] *P. falciparum* NF54 male gametes exflagellation assay at 2 μ M, $n = 2$. [d] Data as published in Reader *et al.* 2021.^[26] ND = not determined.

other modification of the biphenyl (including methoxy- or halogen groups) or replacement thereof, was not tolerated.

Additional *in vitro* lifecycle stage profiling and selectivity

Discovery of antimalarial compounds requires interrogation of multiple life cycle stages of the *P. falciparum* parasite, to profile a compound with specific target candidate profiles (TCP).^[39] This includes compounds with asexual blood stage activity (TCP-1) as well as transmission-blocking compounds (TCP-5). We therefore profiled gametocytocidal hit amides and sulfonamides for additional life cycle stage activity (Table 3). None of the compounds that was active ($IC_{50} < 600$ nM) against late-stage gametocytes showed any appreciable activity on drug sensitive (*P. falciparum* NF54 strain) asexual blood stage parasites at this concentration, on the same assay platform that measures metabolic activity as an indicator of cellular viability (PrestoBlue[®] assay) (Table 3). Cross-validation of this lack of activity with an independent assay that measures cellular proliferation (SYBR Green I fluorescence assay) indicated that <20% inhibition of asexual blood stage proliferation could be obtained at 10 μ M (Table 3). Since assay platform variability can therefore be excluded,^[40] the higher efficacy against late-stage gametocytes points towards a selectivity for transmission-blocking activity, with these compounds >20-fold more potent on late-stage gametocytes compared to asexual blood stage parasites. This propensity of selectivity towards transmission-blocking activity has also been confirmed for ML324^[25,26] and JIB-04,^[25] which may suggest that compounds like 7 may act similarly.

The majority of these compounds displayed >30% inhibition of male gamete exflagellation at 2 μ M (Table 3), similar to other compounds with potent transmission-blocking activity as reported before.^[26,41] However, sex-specificity of the compounds cannot currently be excluded and needs to be confirmed on a female gamete formation assay. Ultimately, transmission-blocking activity will be validated in their ability to affect oocyst formation. These data expands current strategies focussed at discovery of TCP-5 targeted compounds, compounds with the ability to selectively target either mature gametocytes^[26,42] or

gametes.^[41] Such compounds are currently being further profiled^[43] as candidates for combination with asexual blood stage actives or potentially for mass screen-and-test applications.^[44–47] Specific targeting of transmission will have an advantage of targeting specific biology associated with transmission, and, together with the fact that the transmissible stages are non-dividing, this should result in a reduction of resistance development. Moreover, by combining a transmission-targeted compound, with asexual blood stage actives, it could prolong the life span of the latter and prevent resistance transmission.^[44–47] No cytotoxicity was observed for five representative derivatives against a human hepatocellular carcinoma line (HepG2) (Table 3).

Metabolic stability in liver microsomes and physicochemical properties

The amides 16, 6, 7, 8 and 9 and sulfonamides 31, 33, were assessed for stability in human (HLM), rat (RLM) and mouse (MLM) microsomes (Table 4). Overall, the compounds showed species-specific metabolic stability with respect to rodents and humans. Whilst the majority of the compounds displayed stability in HLM and MLM, loss of this was observed for the amide 5 and 9 in RLM. Although a sulfonamide with activity against *P. falciparum* gametocytes and good solubility profiles, 33 showed instability in all three microsomal backgrounds; with 31 also rather instable, which may point to a general challenge

Table 4. *In vitro* microsomal stability and physicochemical properties of selected compounds.

Cmpd	Microsomal stability [min]			Solubility [μ M] pH 6.5
	HLM	RLM	MLM	
16	150	150	150	175
5	150	99.8	119	10
7	150	150	106	10
8	150	150	150	80
9	150	89	150	5
31	88	150	74	135
33	3.43	3.59	3.55	165

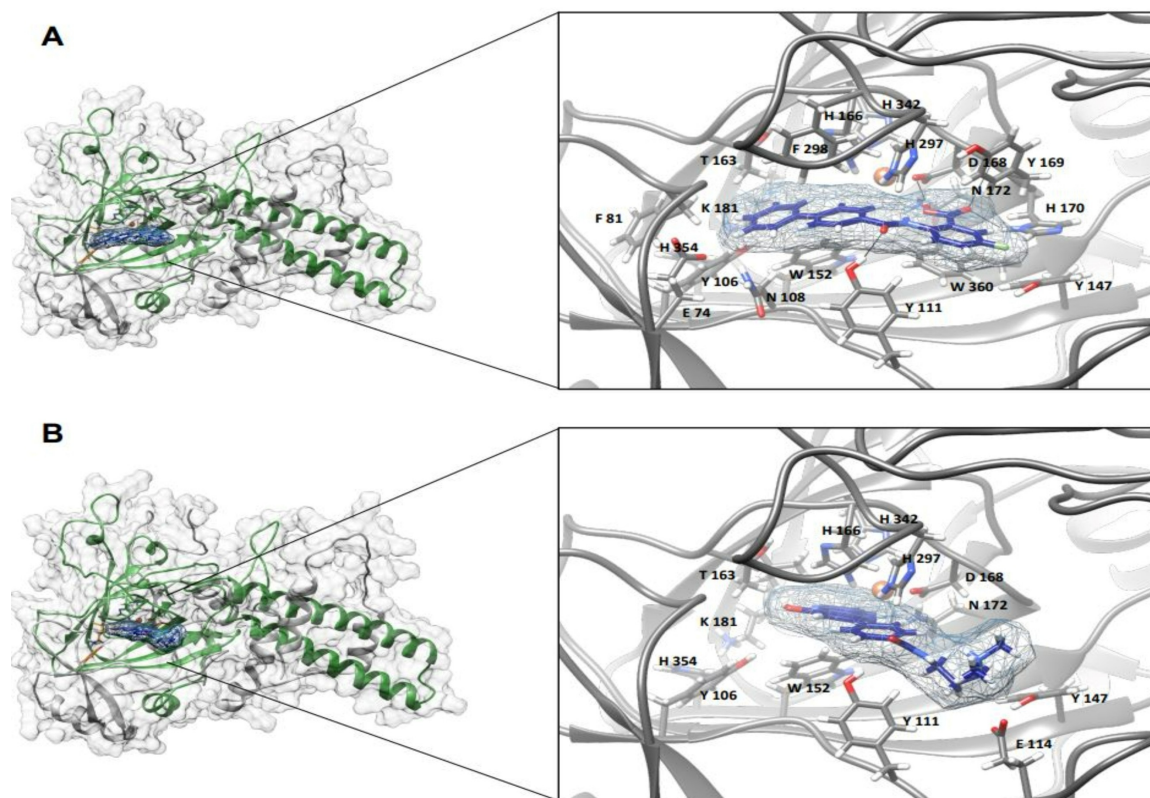


Figure 2. Predicted occlusion of the *Pfjmj3* active site by **7**. Protein models for *Pfjmj3* were generated with AlphaFold2 for *P. falciparum* histone demethylase *jmj3* (accession code Q8IIIE4 PLAF7) with the core *jmj* domains indicated in green. (A) The structure of *Pfjmj3* (with *jmj* domain indicated in green) with **7** (blue) docked into the active site and (B) ML324 as control compound. Active site residues H_{166} , D_{168} and H_{342} coordinates the Fe^{2+} cofactor and Y_{106} , N_{172} and K_{181} the α -KG co-substrate. Hydrogen bonds are indicated in black.

of metabolic instability seen for the sulfonamide derivatives. Unfortunately, the most active, **7**, shows solubility issues but this is overcome in **16**. The 5-fold loss in activity in **16** still presents acceptable potency at < 100 nM with the additional gain in solubility profiles. The latter could be associated with methylation of the phenyl groups on R^4 and R^2 from **7** to **16**. This presents a new scaffold for hit-to-lead optimizations.

Mechanistic evaluation of activity

To understand the activity of the most active amide, **7**, in more detail, the compound was evaluated for its proposed binding to the KDM4B homologue, *Pfjmj3*. Docking of the compound into the *Pfjmj3* active site revealed occlusion of residues involved in the coordination of the Fe^{2+} cofactor (H_{166} , D_{168} and H_{342}) and the α -KG co-substrate (Y_{106} , N_{172} and K_{181}) and this could preclude enzyme function by preventing the formation of iron and succinate intermediates by oxidative decarboxylation^[35] (Figure 2). This was similar in binding to ML324 as key inhibitor (Figure 2) and predicts that *Pfjmj3* could be targeted by **7** in the parasite. Moreover, the amide linker of **7** seems important for specificity, enabling H-bonding with Y_{111} . Since no direct matched sulfonamide pair for **7** is available, we cannot

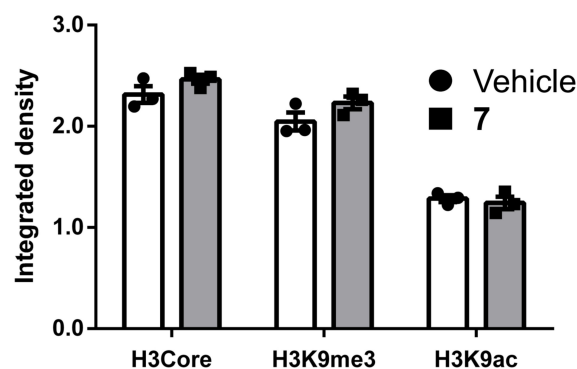


Figure 3. Evaluation of histone methylation levels in **7**-treated late-stage gametocytes of *P. falciparum*. Gametocytes were treated with compound for 24 h after which histone PTM levels were determined by quantitative western dot-blot with antibodies against H3core, H3K9me3 and H3K9ac, compared to vehicle controls. Data are from three independent biological controls, in technical triplicates, means \pm S.E. shown.

determine how the sulfonamide linker will affect this binding mode.

Inhibition of *Pfjmj3* leads to hypermethylation of particularly H3K9me3, as was evident with ML324 action on late-stage gametocytes.^[26] To validate the above predicted inhibition of *Pfjmj3* by **7**, a similar increase in H3K9me3 could be expected.

However, only a marginal increase in H3K9me3 levels was observed in late-stage gametocytes treated with **7** (Figure 3). This contrasts with the ~1.5x increase in methylation of H3K9me3 seen after ML324 treatment.^[26] Whilst we do not have evidence for potential hypermethylation at other histone marks (e.g. H3K36me3), this indicates that the potent effect seen with **7** may be as a result of additional (off-target) effects in gametocytes, dissimilar to the effect of ML324.

Conclusion

Here, we designed and synthesized a novel set of 2-(arylcaboxamido)benzoic acid, 2-(arylsulfonamido)benzoic acid and *N*-(2-(1*H*-tetrazol-5-yl)phenyl)-arylcaboxamide derivatives as part of a hit-to-lead optimization program. We identified *P. falciparum* gametocyte specific compounds with activity on both late-stage gametocytes as well as male gametes, emphasizing the potential for these compounds to have transmission-blocking activity. Mechanistic evaluation of the most active amide compound (**7**) could not confirm hypermethylation of particularly H3K9me3, as seen with other malaria Jumonji enzyme inhibitors such as ML324. However, *Pfjnj3* is the direct homologue of several *jmj*-containing mammalian enzymes and this supports the selection of these compounds from a library intended for mammalian KDM4B inhibition based on structure-based analogue design.

Experimental Section

Chemistry: All 2-(arylcaboxamido)benzoic acid, 2-(arylsulfonamido)benzoic acid and *N*-(2-(1*H*-tetrazol-5-yl)phenyl)-arylcaboxamide derivatives were synthesized as previously described.^[34] All intermediates and target compounds were purified by silica gel or C18 column chromatography. Pure intermediates and final products were fully characterized by NMR and LC-MS analysis (Supporting Information). Purity of intermediates and final products was determined by UPLC analysis, and final compounds were $\geq 95\%$ pure prior to use in biological studies.

***In vitro* cultivation of *P. falciparum* asexual parasites and gametocytes:** All *in vitro* experiments involving human blood donors and human malaria parasites holds ethics approval from the University of Pretoria Research Health Sciences Ethics Committee (506/2018) and Natural and Agricultural Sciences Ethics Committee (NAS 18000094). This work abides by the Declaration of Helsinki principles.

Intra-erythrocytic asexual *P. falciparum* parasites (NF54 strain, drug-sensitive) was cultivated in fresh human erythrocytes (either A⁺ or O⁺) in RPMI-1640 culture medium supplemented with 25 mM HEPES (pH 7.5, Sigma Aldrich, USA), 0.2 mM hypoxanthine (Sigma Aldrich, USA), 0.024 $\mu\text{g}/\mu\text{L}$ gentamycin (Hyclone, USA), 5 $\mu\text{g}/\mu\text{L}$ Albumax II (Invitrogen, USA), 23.81 mM sodium bicarbonate (Sigma Aldrich, USA) and 0.2% (w/v) D-glucose. Cultures were maintained with daily media change and fresh erythrocyte supplementation at 5% haematocrit, 2% parasitaemia under hypoxic conditions (5% O₂, 5% CO₂, 90% N₂) with moderate shaking at 37 °C. Parasites were synchronized to more than 90% rings stages with 5% (w/v) D-sorbitol. Gametocytogenesis production was initiated at 0.5% parasitaemia and a 6% haematocrit in a glucose-free medium

under hypoxic gaseous (5% O₂, 5% CO₂, 90% N₂) conditions at 37 °C without shaking.^[40] The haematocrit was reduced to 4% after 72 h, mimicking anaemic conditions in the patient. Asexual parasites were eliminated from the cultures following gametocytogenesis by the addition of 50 mM *N*-acetyl glucosamine (NAG) at day 3–7.^[26]

Antiplasmodium activity evaluation: Compounds were screened against NF54 *P. falciparum* *in vitro* using both the PrestoBlue[®] and the SYBR Green I fluorescence assays as previously described.^[26,48] Briefly, to allow for direct comparison between the asexual and sexual stage activity, the same PrestoBlue[®] platform was used. Synchronized trophozoite stages (*PfNF54*, 2% parasitaemia, 5% haematocrit, 100 $\mu\text{L}/\text{well}$) were incubated in the presence of various concentrations of compounds at 37 °C for 48 h under hypoxic conditions, and the PrestoBlue[®] performed as before. Dihydroartemisinin (DHA) was used as positive kill control. All assays were performed for three independent biological replicates in technical triplicates. The SYBR green I assay was performed on synchronized *in vitro PfNF54* ring stage parasites (1% parasitaemia, 1% haematocrit) under drug pressure for 96 h. Chloroquine was used baseline background control and the fluorescence determined as described. Data are for three independent biological replicates in technical triplicates.

Stage IV/V gametocyte cultures (*PfNF54*, 2% parasitaemia, 5% haematocrit, 100 $\mu\text{L}/\text{well}$) were exposed to compounds and incubated at 37 °C for 48 h under hypoxic conditions and the PrestoBlue[®] assay performed as before^[40] on three independent biological replicates with DHA as control. All data was performed using GraphPad Prism (v6).

Male gamete exflagellation assay: Mature *PfNF54* gametocytes (> 95% stage V) were treated with 2 μM compound in complete culture media (final DMSO concentration of <0.1% (v/v)) for 48 h at 37 °C under hypoxic conditions. Gametogenesis was induced by exposing the mature gametocytes to ookinete media [RPMI-1640 media (Sigma-Aldrich) supplemented with 25 mM HEPES, 0.2% (w/v) sodium bicarbonate, pH 8.0, 50% (v/v) human serum, and 100 μM xanthurenic acid] at room temperature for 16 min. The inhibition of exflagellation was measured through drug pressure carry over as previously described,^[26,49] including methylene blue as the reference control for inhibition of male exflagellation. Exflagellating centres were detected by video microscopy (Carl Zeiss NT 6V/10W Stab 480 microscope with a MicroCapture camera, 10 \times magnification) in a Neubauer chamber at room temperature and semi-automatically quantified after 24 min from 16 randomly located fields from which videos of 8–10 s each were taken at 30 s intervals. The total exflagellating centres per treatment were quantified using ICY (open-source imaging software GPLv3) normalised to an untreated control. Assays were performed for two biological repeats.

Cytotoxicity evaluation: The *in vitro* cytotoxicity was evaluated against human Caucasian hepatocellular carcinoma cells (HepG2) as previously described.^[50] Cells were cultivated *in vitro* in complete DMEM media (Hyclone, U.S.A.) supplemented with 10% (v/v) heat inactivated foetal bovine serum and 1% (v/v) penicillin/streptomycin at 37 °C in 5% CO₂. Cells were detached with 0.25% (v/v) Trypsin-EDTA once ~80% confluency was observed,^[51] and cell viability was monitored microscopically with 0.2% (w/v) Trypan-Blue using a Neubauer chamber. Cells were seeded into 96-well plates (2×10^4 cells/well) and incubated overnight at 37 °C under 5% CO₂ and 95% humidity. Following incubation, cells were exposed to a serial dilution range of the compounds under investigation. Cytotoxicity was then determined using the lactate dehydrogenase release assay using the CytoSelect™ LDH Cytotox-

icity Assay Kit with absorbance measured at 450 nm. Data were obtained for a single biological repeat in technical triplicates.

In vitro hepatic microsomal stability: The metabolic stability assay was performed using a single-point metabolic stability assay.^[52] Briefly, the compounds were incubated at 1 μ M in human (mixed gender, Xenotech), rat (male rat IGS, Xenotech) and mouse (male mouse CD1, Xenotech) liver microsomes (0.4 mg/mL) for 30 min at 37 °C. Reactions were quenched by adding ice-cold acetonitrile containing internal standard. The samples were then centrifuged and analysed by LC-MS/MS for the disappearance of parent compound. Half-life, clearance and hepatic excretion ratios were determined using standard equations.^[52,53]

Kinetic solubility: Solubility was measured at pH 6.5 using an adapted miniaturised shake-flask method, in 96-well plate format.^[54] Briefly 4 μ L of a 10 mM stock in DMSO was added to a 96-well plate and evaporated using a GeneVac system. Phosphate buffer pH 6.5 was then added to the wells and the plate was incubated for 24 h at 25 °C with shaking. At the end of this incubation, the samples were centrifuged at 3500 g for 15 min then transferred to an analysis plate. A calibration curve in DMSO for each sample between 10–220 μ M was prepared and included in the analysis plate. Analysis was then performed by HPLC-DAD and solubility of each sample determined from the corresponding calibration curve.^[55]

Molecular docking: A model of Pflmj3 was obtained from DeepMind's AlphaFold2 (www.alphafold.ebi.ac.uk) *P. falciparum* protein structure repository.^[56] Structural assessment of the model structure was performed using MolProbity v. 4.5.1 (<https://molprobity.biochem.duke.edu>) and InterPro (<https://www.ebi.ac.uk/interpro>) was used to identify relevant protein features. Docking of the ligand to Pflmj3 was evaluated using SwissDock^[57,58] and binding modes were visualised using the ViewDock utility of UCSF Chimera 1.15 and LigPlot+.

Immunoblot evaluation of histone tail methylation: Late-stage gametocytes (stage IV/V) were treated with **7** at 5 μ M for 24 h. Thereafter, histones were extracted and enriched, as previously described.^[26] Briefly, gametocytes were released from the erythrocyte compartment using 0.06% saponin and parasite nuclei isolated in a hypotonic lysis buffer in the presence of protease inhibitor cocktail by homogenisation. Histones were acid extracted overnight at 4 °C and precipitated in 20% trichloroacetic acid. Histone samples were quantitatively spotted onto nitrocellulose membranes in triplicate, the membranes blocked in 5% blotting-grade blocker (Bio-Rad) in TBS-tween for 1 h. Histone marks were probed overnight with α -H3K9me3 (Abcam ab8898, 1:10 000), α -H3K9ac (Abcam ab4441, 1:10,000) and α -H3 core (Abcam ab6721, 1:10,000) antibodies followed by detection with a horseradish peroxidase-conjugated goat α -rabbit secondary antibody (Abcam ab6721, 1:5 000) and signal visualised with Pierce SuperSignal West Pico PLUS Chemiluminescent Substrate. ImageJ 1.52n was used to determine integrated density of treated and vehicle control samples ($n = 3, \pm$ S.E.).

Acknowledgements

We appreciate Suzan Maboane's technical assistance. The authors would also like to acknowledge the H3D Drug Discovery and Development Centre at UCT for the microsomal stability and solubility data. This work was supported by the South African Medical Research Council Strategic Health Innovation Partnership and the Department of Science and Innovation South African

Research Chairs Initiative, administered through the South African National Research Foundation (UID 84627) and a BMGF Grand Challenges Africa grant (GCA/DD2/Round10/021/001) to LMB. The UP ISMC acknowledges the South African Medical Research Council (SA MRC) as Collaborating Centre for Malaria Research. All compounds evaluated in the manuscript were selected from a chemical library originally synthesized for another project funded by 1R01 DE 029637 (PMW). A portion of the work described herein was supported by the South Carolina SmartState® Endowed Chair for Drug Discovery.

Conflict of Interest

The authors declare no conflict of interest.

Data Availability Statement

The data that support the findings of this study are available from the corresponding author upon reasonable request.

Keywords: antimalarials · epigenetics · gametocytes · heterocycles · inhibitors · Plasmodium

- [1] D. Dhanak, P. Jackson, *Biochem. Biophys. Res. Commun.* **2014**, *455*, 58–69.
- [2] J. E. Audia, R. M. Campbell, *Cold Spring Harbor Perspect. Biol.* **2016**, *8*, a019521.
- [3] W. Sun, T. Q. Tanaka, C. T. Magle, W. Huang, N. Southall, R. Huang, S. J. Dehdashti, J. C. McKew, K. C. Williamson, W. Zheng, *Sci. Rep.* **2014**, *4*, 3743.
- [4] J. A. Engel, A. J. Jones, V. M. Avery, S. D. Sumanadasa, S. S. Ng, D. P. Fairlie, T. S. Adams, K. T. Andrews, *Int. J. Parasitol.* **2015**, *5*, 117–126.
- [5] L. M. Birkholtz, T. L. Coetzer, D. Mancama, D. Leroy, P. Alano, *Trends Parasitol.* **2016**, *32*, 669–681.
- [6] M. E. van der Watt, J. Reader, L. M. Birkholtz, *Front. Cell. Infect. Microbiol.* **2022**, *12*, 901971.
- [7] N. Coetzee, S. Sidoli, R. van Biljon, H. Painter, M. Llinas, B. A. Garcia, L. M. Birkholtz, *Sci. Rep.* **2017**, *7*, 607.
- [8] J. Connacher, H. von Grüning, L. Birkholtz, *Front. Cell Dev. Biol.* **2022**.
- [9] S. Abel, K. G. Le Roch, *Brief Funct. Gen.* **2019**.
- [10] A. P. Gupta, Z. Bozdech, *Int. J. Parasitol.* **2017**, *47*, 399–407.
- [11] M. T. Duraisingh, K. M. Skillman, *Annu. Rev. Microbiol.* **2018**, *72*, 355–375.
- [12] A. Cortes, K. W. Deitsch, *Cold Spring Harbor Perspect. Med.* **2017**, *7*.
- [13] A. M. Salcedo-Amaya, W. A. Hoeijmakers, R. Bartfai, H. G. Stunnenberg, *Int. J. Biochem. Cell Biol.* **2010**, *42*, 781–784.
- [14] K. Trenholme, L. Marek, S. Duffy, G. Pradel, G. Fisher, F. K. Hansen, T. S. Skinner-Adams, A. Butterworth, C. J. Ngwa, J. Moecking, C. D. Goodman, G. I. McFadden, S. D. Sumanadasa, D. P. Fairlie, V. M. Avery, T. Kurz, K. T. Andrews, *Antimicrob. Agents Chemother.* **2014**, *58*, 3666–3678.
- [15] A. Bouchut, D. Rotili, C. Pierrot, S. Valente, S. Lafitte, J. Schultz, U. Hoglund, R. Mazzone, A. Lucidi, G. Fabrizi, D. Pechalrieu, P. B. Arimondo, T. S. Skinner-Adams, M. J. Chua, K. T. Andrews, A. Mai, J. Khalife, *Eur. J. Med. Chem.* **2019**, *161*, 277–291.
- [16] N. A. Malmquist, T. A. Moss, S. Mecheri, A. Scherf, M. J. Fuchter, *Proc. Natl. Acad. Sci. USA* **2012**, *109*, 16708–16713.
- [17] N. A. Malmquist, S. Sundriyal, J. Caron, P. Chen, B. Witkowski, D. Menard, R. Suwanarusk, L. Renia, F. Nosten, M. B. Jimenez-Diaz, I. Angulo-Barturen, M. S. Martinez, S. Ferrer, L. M. Sanz, F. J. Gamo, S. Wittlin, S. Duffy, V. M. Avery, A. Ruecker, M. J. Delves, R. E. Sinden, M. J. Fuchter, A. Scherf, *Antimicrob. Agents Chemother.* **2015**, *59*, 950–959.
- [18] V. Chua, M. Orloff, J. L. Teh, T. Sugase, C. Liao, T. J. Purwin, B. Q. Lam, M. Terai, G. Ambrosini, R. D. Carvajal, G. Schwartz, T. Sato, A. E. Aplin, *EMBO Mol. Med.* **2019**, *11*.

- [19] S. Sundriyal, P. B. Chen, A. S. Lubin, G. A. Lueg, F. Li, A. J. P. White, N. A. Malmquist, M. Vedadi, A. Scherf, M. J. Fuchter, *MedChemComm* **2017**, *8*, 1069–1092.
- [20] D. Prusty, P. Mehra, S. Srivastava, A. V. Shivange, A. Gupta, N. Roy, S. K. Dhar, *FEMS Microbiol. Lett.* **2008**, *282*, 266–272.
- [21] K. T. Andrews, T. N. Tran, N. C. Wheatley, D. P. Fairlie, *Curr. Top. Med. Chem.* **2009**, *9*, 292–308.
- [22] K. T. Andrews, A. P. Gupta, T. N. Tran, D. P. Fairlie, G. N. Gobert, Z. Bozdech, *PLoS One* **2012**, *7*, e31847.
- [23] N. Coetzee, H. von Gruning, D. Opperman, M. van der Watt, J. Reader, L. M. Birkholtz, *Sci. Rep.* **2020**, *10*, 1–11.
- [24] L. N. Vanheer, H. Zhang, G. Lin, B. F. C. Kafsack, *Antimicrob. Agents Chemother.* **2020**, *64*.
- [25] K. A. Matthews, K. M. Senagbe, C. Notzel, C. A. Gonzales, X. Tong, F. Rijo-Ferreira, N. V. Bhanu, C. Miguel-Blanco, M. J. Lafuente-Monasterio, B. A. Garcia, B. F. C. Kafsack, E. D. Martinez, *ACS Infect. Dis.* **2020**, *6*, 1058–1075.
- [26] J. Reader, M. E. van der Watt, D. Taylor, C. Le Manach, N. Mittal, S. Otilie, A. Theron, P. Moyo, E. Erlank, L. Nardini, N. Venter, S. Lauterbach, B. Bezuidenhout, A. Horatscheck, A. van Heerden, N. J. Spillman, A. N. Cowell, J. Connacher, D. Opperman, L. M. Orchard, M. Llinas, E. S. Istvan, D. E. Goldberg, G. A. Boyle, D. Calvo, D. Mancama, T. L. Coetzee, E. A. Winzeler, J. Duffy, L. L. Koekemoer, G. Basarab, K. Chibale, L. M. Birkholtz, *Nat. Commun.* **2021**, *12*, 269.
- [27] B. K. Chaal, A. P. Gupta, B. D. Wastuwidyaningtyas, Y. H. Luah, Z. Bozdech, *PLoS Pathog.* **2010**, *6*, e1000737.
- [28] J. E. Kirkpatrick, K. L. Kirkwood, P. M. Woster, *Epigenetics* **2018**, *13*, 557–572.
- [29] D. H. Lee, G. W. Kim, Y. H. Jeon, J. Yoo, S. W. Lee, S. H. Kwon, *FASEB J.* **2020**, *34*, 3461–3484.
- [30] L. Cui, Q. Fan, L. Cui, J. Miao, *Int. J. Parasitol.* **2008**, *38*, 1083–1097.
- [31] K. A. Rai, G. Tumber, A. et al., in *Probe Reports from the NIH Molecular Libraries Program*, Bethesda (MD): National Center for Biotechnology Information (US), **2012** Dec 17 [Updated 2013 Sep 16].
- [32] J. E. Kirkpatrick, K. L. Kirkwood, P. M. Woster, *Epigenetics* **2018**, *13*, 557–572.
- [33] S. Saurav Pathak, S. Maitra, S. Chakravarty, A. Kumar, *Histone Lysine Demethylases of JMJD2 or KDM4 Family are Important Epigenetic Regulators in Reward Circuitry in the Etiopathology of Depression*, Vol. 42, **2016**.
- [34] C. M. Mills, J. M. Turner, I. C. Piña, K. A. Garrabrant, D. Geerts, A. S. Bachmann, Y. K. Peterson, P. M. Woster, *Eur. J. Med. Chem.* **2022**, *234*, ePub ahead of print.
- [35] K. A. Matthews, K. M. Senagbe, C. Notzel, C. A. Gonzalez, X. Tong, F. Rijo-Ferreira, B. V. Natarajan, C. Miguel-Blanco, M. J. Lafuente-Monasterio, B. A. Garcia, *ACS Infect. Dis.* **2020**.
- [36] N. A. Meanwell, *J. Med. Chem.* **2018**, *61*, 5822–5880.
- [37] C. C. Wirth, S. Glushakova, M. Scheuermayer, U. Repnik, S. Garg, D. Schaack, M. M. Kachman, T. Weissbach, J. Zimmerberg, T. Dandekar, G. Griffiths, C. E. Chitnis, S. Singh, R. Fischer, G. Pradel, *Cell. Microbiol.* **2014**, *16*, 709–733.
- [38] J. Reader, M. E. van der Watt, L. M. Birkholtz, *Front. Cell. Infect. Microbiol.* **2022**, *12*, 926460.
- [39] J. N. Burrows, S. Duparc, W. E. Gutteridge, R. Hoof van Huijsduijnen, W. Kaszubska, F. Macintyre, S. Mazzuri, J. J. Mohrle, T. N. C. Wells, *Malar. J.* **2017**, *16*, 26.
- [40] J. Reader, M. Botha, A. Theron, S. B. Lauterbach, C. Rossouw, D. Engelbrecht, M. Wepener, A. Smit, D. Leroy, D. Mancama, T. L. Coetzee, L. M. Birkholtz, *Malar. J.* **2015**, *14*, 213.
- [41] M. J. Delves, C. Miguel-Blanco, H. Matthews, I. Molina, A. Ruecker, S. Yahiya, U. Straschil, M. Abraham, M. L. Leon, O. J. Fischer, A. Rueda-Zubiaurre, J. R. Brandt, A. Cortes, A. Barnard, M. J. Fuchter, F. Calderon, E. A. Winzeler, R. E. Sinden, E. Herreros, F. J. Gamero, J. Baum, *Nat. Commun.* **2018**, *9*, 3805.
- [42] M. Abraham, K. Gagaring, M. L. Martino, M. Vanaerschot, D. M. Plouffe, J. Calla, K. P. Godinez-Macias, A. Y. Du, M. Wree, Y. Antonova-Koch, K. Eribez, M. R. Luth, S. Ottilie, D. A. Fidock, C. W. McNamara, E. A. Winzeler, *ACS Infect. Dis.* **2020**, *6*, 613–628.
- [43] A. Rueda-Zubiaurre, S. Yahiya, O. J. Fischer, X. Hu, C. N. Saunders, S. Sharma, U. Straschil, J. Shen, E. W. Tate, M. J. Delves, J. Baum, A. Barnard, M. J. Fuchter, *J. Med. Chem.* **2020**, *63*, 2240–2262.
- [44] L. Birkholtz, P. Alano, D. Leroy, *Trends Parasitol.* **2022**, *38*, 390–403.
- [45] M. J. Delves, F. Angrisano, A. M. Blagborough, *Trends Parasitol.* **2018**, *34*, 735–746.
- [46] R. E. Sinden, *PLoS Pathog.* **2017**, *13*, e1006336.
- [47] R. E. Sinden, *Adv. Parasitol.* **2017**, *97*, 147–185.
- [48] M. Leshabane, G. A. Dziwornu, D. Coertzen, J. Reader, P. Moyo, M. van der Watt, K. Chisanga, C. Nsanzubuhoro, R. Ferger, E. Erlank, N. Venter, L. Koekemoer, K. Chibale, L. M. Birkholtz, *ACS Infect. Dis.* **2021**, *7*, 1945–1955.
- [49] N. Coetzee, H. von Gruning, D. Opperman, M. van der Watt, J. Reader, L. M. Birkholtz, *Sci. Rep.* **2020**, *10*, 2355.
- [50] B. K. Verlinden, J. Niemand, J. Snyman, S. K. Sharma, R. J. Beattie, P. M. Woster, L. M. Birkholtz, *J. Med. Chem.* **2011**, *54*, 6624–6633.
- [51] D. Coertzen, J. Reader, M. van der Watt, S. H. Nondaba, L. Gibhard, L. Wiesner, P. Smith, S. D'Alessandro, D. Taramelli, H. N. Wong, J. L. du Preez, R. W. K. Wu, L. M. Birkholtz, R. K. Haynes, *Antimicrob. Agents Chemother.* **2018**, *62*.
- [52] L. Di, E. H. Kerns, N. Gao, S. Q. Li, Y. Huang, J. L. Bourassa, D. M. Huryn, *J. Pharm. Sci.* **2004**, *93*, 1537–1544.
- [53] R. S. Obach, *Drug Metab. Dispos.* **1999**, *27*, 1350–1359.
- [54] L. Zhou, L. Yang, S. Tilton, J. Wang, *J. Pharm. Sci.* **2007**, *96*, 3052–3071.
- [55] L. Di, E. H. Kerns, G. T. Carter, *Curr. Pharm. Des.* **2009**, *15*, 2184–2194.
- [56] J. Jumper, R. Evans, A. Pritzel, T. Green, M. Figurnov, O. Ronneberger, K. Tunyasuvunakool, R. Bates, A. Židek, A. Potapenko, *Nature* **2021**, *596*, 583–589.
- [57] A. Grosdidier, V. Zoete, O. Michielin, *J. Comput. Chem.* **2011**, *32*, 2149–2159.
- [58] A. Grosdidier, V. Zoete, O. Michielin, *Nucleic Acids Res.* **2011**, *39*, W270–W277.

Manuscript received: July 27, 2022

Revised manuscript received: September 14, 2022

Accepted manuscript online: September 15, 2022

Version of record online: October 6, 2022